Influence of Ni on Cu precipitation in Fe–Cu–Ni ternary alloy by an atomic study*

Zhu Lu-Shan(朱露珊) and Zhao Shi-Jin(赵世金)†

Key Laboratory for Microstructures, Institute of Materials Science, School of Materials Science and Engineering, Shanghai University, Shanghai 200072, *China*

(Received 20 October 2013; revised manuscript received 12 December 2013; published online 10 April 2014)

The early aging Cu precipitations in Fe–3%Cu and Fe–3%Cu–4%Ni ternary alloys are investigated by molecular dynamics (MD) simulations. The results show that the average size of Cu clusters in Fe–3%Cu–4%Ni alloy is larger than that in Fe–3%Cu alloy. The diffusion of Cu is accelerated by Ni according to the mean square displacement (MSD). Furthermore, the whole formation process of Cu-rich clusters is analyzed in detail, and it is found that the presence of Ni promotes small Cu-rich clusters to be combined into big ones. Ni atoms prefer to stay at the combination positions of small clusters energetically due to a large number of the first nearest neighbor Cu–Ni interactions, which is verified by first-principles calculations based on density functional theory (DFT).

Keywords: Cu precipitation, Fe–Cu–Ni ternary alloy, molecular dynamics, first-principles calculations

PACS: 36.40.−c, 61.82.Bg, 02.70.Ns, 31.15.E− **DOI:** 10.1088/1674-1056/23/6/063601

1. Introduction

Cu-rich precipitation plays an important role in the hardening of high-strength low-alloy (HSLA) steels.[1,2] However, the origin of embrittlement of ferritic steel used as structural material for pressure vessels of nuclear reactors (RPV) is also confirmed.[3,4] The Cu precipitation and relevant basic mechanism are of fundamental scientific interest. Experimentally, extensive studies on the structural, compositional, and morphological evolutions of Cu precipitates have been carried out by using a variety of microstructural techniques, including atom probe tomography (APT).[5–11] Theoretically, multiscale simulations focused on the formation and evolution of Cu-rich clusters or precipitates, phase transition, interactions between Cu clusters and vacancies, ripening processes, and Cu diffusion in Fe-matrix.[12–19]

Cu precipitates consist of Cu, Ni, and other foreign atoms. Cu and Ni are phenomenologically considered to be the main elements responsible for steel hardening and embrittlement. Ni is presented initially in the particles, but it is prone to be segregated from the core of Cu-rich precipitates to the interface of Cu-rich precipitates and matrix at the growth and coarsening stages.[20,21] Ni, as the third-party element, has much influence on Cu precipitation. Investigations have shown that the addition of Ni into Fe–Cu alloy accelerates Cu precipitation,[22] increases the nucleation rate and increases the number of Cu particles.[23] Al-Motasem *et al.*[24] revealed that Cu_mNi_n clusters have lower formation energy than the pure Cu clusters. Seko *et al.*[25] provided a similar result using *ab-initio* calculation. A latest research paper has exposed that Ni has a temporal delay effect on Cu precipitation by reducing the diffusion coefficient of Cu clusters at the coarsening stage.[26] However, there are few intuitive reports about the specific behaviors of Ni atoms that contribute to promoting Cu precipitation at an atomic scale.

Molecular dynamics (MD) simulations are widely used in the study of structures, energy, and phase transformation, and can give some insight into the kinetic properties of precipitation, which is very difficult to obtain from experiments. First-principles calculations based on density functional theory (DFT) have been proved to be a very accurate tool in describing various material properties. In this work, MD simulations are used to analyze the formation process of Cu-rich clusters in Fe–Cu–Ni ternary alloy and to study the influence of Ni on Cu precipitation. The results of MD simulations are also verified by first-principles calculations with good reliability. The rest of this article is organized as follows. The calculation details are presented in Section 2. The influence of Ni on Cu precipitation and the formation of Cu-rich clusters are analyzed in Section 3. The results are summarized in Section 4.

2. Calculation details

2.1. Molecular dynamics simulation details

MD simulation in combination with a reasonable potential function is a rather powerful approach to the modeling of Cu precipitation at an early stage. An embedded-atom method (EAM) potential developed by Bonny *et al.*[27] is used in this work, which can well describe the alloy thermodynamic properties and the interactions between solute atoms and point-defects. The Cu solubility in body-centered cubic (bcc) Fe of

*Project supported by the National Natural Science Foundation of China (Grant Nos. 50931003 and 51301102) and the 085 Project at Shanghai University, China.

†Corresponding author. E-mail: shijin.zhao@shu.edu.cn

© 2014 Chinese Physical Society and IOP Publishing Ltd

this ternary potential for true thermodynamic phases in equilibrium follows the experimental results reasonably in the temperature range which is of interest to experiment.

Since the diffusion of Cu was slow, the Cu-rich clusters should be observed to take a long time in RPV model steel with a composition of 1.07 at.% Cu and 1.95 at.% Ni in previous MD simulations. Therefore, Fe–3%Cu and Fe–3%Cu–4%Ni (at.%) alloys with high concentrations of Cu and Ni were simulated at 823 K and 1100 K. Fe–3%Cu and Fe–3%Cu–4%Ni alloys were adopted to investigate the influence of Ni on Cu-rich cluster formation comparatively. The two alloys with 0.1 at.% vacancy concentration were considered. The MD simulations were carried out in crystallites with $20 \times 20 \times 20$ lattice unit cubic cells (1.6×10^4 lattice sites), and the lattice constant was 2.855 Å. To avoid the effects of free surfaces on the simulated array, the periodic boundary conditions were applied to three directions of MD cells. Prior to each simulation, Cu, Ni atoms and vacancies were randomly distributed over the lattice positions of the crystallite till the desired proportions were reached. An energy minimization procedure was performed with a steepest descent algorithm on every initial structure to obtain the equilibrium structure of systems. The simulation models were fully relaxed by 2×10^5 steps with NPT ensemble which was at the desired temperature under zero-pressure state. Subsequently, simulations were carried out with NVT ensemble under the same temperature and pressure conditions for 1×10^8 steps. The MD time step was 2 fs.

The MD simulations were performed by making use of the large-scale atomic/molecular massively parallel simulator (LAMMPS) code[28] and the results were visualized by visual molecular dynamics (VMD).[29] In order to distinguish whether Cu and Ni atoms belong to Cu-rich clusters intuitively, the dynamic bonds were applied to the snapshots by setting the cut-off radius to be 4.0 Å. This value was determined by the third nearest neighbor interactions of Cu. That is, atoms whose interatomic distances were less than 4.0 Å were considered to have interatomic interactions and to form Cu-rich clusters.

2.2. First-principles calculation details

First-principles calculations were performed to verify the effect of Ni on Cu precipitation which was obtained by MD simulations. This method was based on DFT[30] using a plane wave basis and solving the Kohn–Sham equation[31] in the Vienna *ab initio* simulation package (VASP).[32] All calculations of electronic structure and total energies were performed within the projector augmented wave (PAW) formalism with the generalized gradient approximation (GGA) for the functional exchange.[33–35] Spin polarization was considered for the ferromagnetic Fe–Cu–Ni ternary alloy. Cu clusters and Ni atoms with different configurations in the $3 \times 3 \times 3$ conventional bcc Fe unit cells (54 lattice sites) were calculated with $4 \times 4 \times 4$ k-points. An energy cut-off of 350 eV was used in all cases. The structural relaxations of the ions were calculated by conjugate-gradient (CG) algorithm.

3. Results and discussion

3.1. Molecular dynamics simulations

The MD simulations of Fe–3%Cu and Fe–3%Cu–4%Ni alloys, both aging at 823 K and 1100 K, were conducted. The Cu diffusivity D^* (at a given temperature and vacancy concentration) in bcc Fe-matrix can be calculated according to the following equation,[36,37]

$$D^* = \frac{\langle R^2(t) \rangle}{6t}, \tag{1}$$

where t is the simulation time and $\langle R^2(t) \rangle$ is the mean square displacement (MSD) of Cu atoms as a function of time. The MSD is defined as

$$\langle R^2(t) \rangle = \frac{\sum_j^{N_{\mathrm{Cu}}} (r_j(t) - r_j(0))^2}{N_{\mathrm{Cu}}}, \tag{2}$$

where N is the number of the calculated element Cu atoms in the computational box, $r_j(t)$ is the location of the j-th Cu atom at time t, $\langle R^2(t) \rangle$ is averaged over 500-MD-time intervals (1 ps per interval). D^* could be calculated after sufficiently long time simulations.

In Fig. 1, it can be clearly observed that linear trends exist and the Cu diffusion coefficients can be directly estimated. The maximum MSD values of Cu atoms in Fe–3%Cu and Fe–3%Cu–4%Ni alloys are, respectively, 27 Å^2 and 38 Å^2 for the alloys aging at 823 K, and 229 Å^2 and 321 Å^2 for the alloys aging at 1100 K. The diffusion of Cu increases significantly with the increase of temperature, which can be easily understood because the atoms move more dramatically at higher temperatures. Notably, Cu diffusion coefficients are larger in Fe–3%Cu–4%Ni alloys than in Fe–3%Cu alloys for their aging at both 823 K and 1100 K, which indicates that the diffusion of Cu is accelerated by Ni.

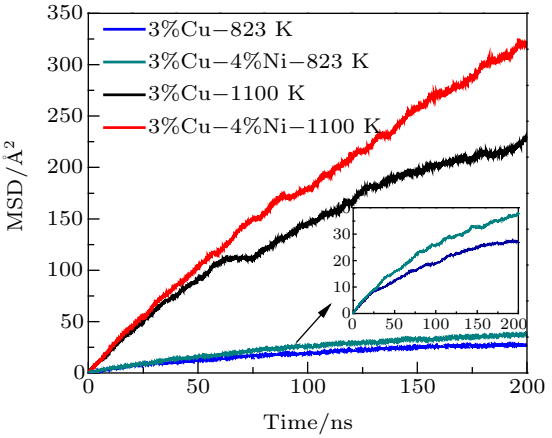


Fig. 1. (color online) MSDs of Cu-atom of Fe–3%Cu and Fe–3%Cu–4%Ni alloys aging at 823 K and 1100 K. The inset shows the magnified parts of MSDs of Fe–3%Cu and Fe–3%-Cu4%Ni aging at 823 K.

The numbers of Cu clusters containing more than 6 Cu atoms in Fe–3%Cu alloys and Fe–3%Cu–4%Ni alloys are shown in Fig. 2. The numbers of Cu clusters containing $6 \sim 10$ and more than 15 Cu atoms are 14 and 0 in Fe–3%Cu alloy aging at 823 K, respectively. Furthermore, a larger number of Cu clusters containing more than 20 Cu atoms is found in Fe–3%Cu–4%Ni alloy aging at 1100 K. The average sizes of Cu clusters in Fe–3%Cu alloy and Fe–3%Cu–4%Ni alloy are 8.1, 11.1 Cu atoms per cluster for the alloys aging at 823 K and 10.7, 13.8 Cu atoms per cluster for the alloys aging at 1100 K, respectively. Summing up the average size of Cu clusters, it is found that the size of Cu clusters in Fe–3%Cu–4%Ni alloy is larger than in Fe–3%Cu alloys for their aging at both 823 K and 1100 K. The largest Cu cluster contains $30 \sim 35$ Cu atoms of which the diameter is about 1.7 nm in Fe–3%Cu–4%Ni alloy aging at 1100 K. The average size of a Cu cluster increases obviously due to the presence of Ni. As discussed before, the diffusion of Cu is accelerated by Ni. However, this is only one of the factors that are conductive to Cu precipitation. The cohesive energies of Cu and Ni are 3.49 eV/atom and 4.44 eV/atom, respectively,[38] which indicates that the structure of Ni cluster is more stable than that of Cu cluster. It is confirmed that Cu clusters formed in Fe–3%Cu–4%Ni alloys are more stable and so grow into large clusters because of the addition of Ni. In order to deeply expounding the influence of Ni on the formation of Cu-rich cluster, the specific behaviors of Ni will be further discussed later in this section.

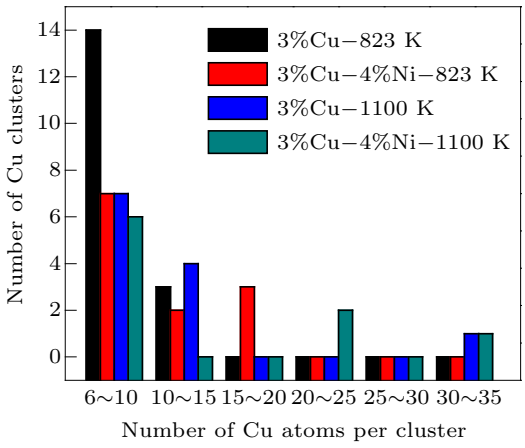


Fig. 2. (color online) Variations of the number of Cu clusters with the number of Cu atoms contained for Fe–3%Cu and Fe–3%Cu–4%Ni alloys aging at 823 K and 1100 K.

Fe–3%Cu–4%Ni alloy aging at 1100 K is chosen to analyze the formation of Cu-rich cluster and the specific behaviors of Ni in the following. A few clusters form and annihilate during the whole simulation. The absence of these tiny clusters can be due to their sizes, which are too small to be resolved above the random fluctuations. Figure 3 shows that Cu clusters stably remain at the end of aging process ($t = 200$ ns). The Cu-rich clusters with large size exhibit the ellipoidal shapes.

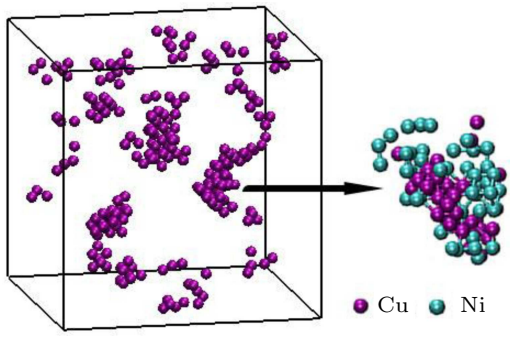


Fig. 3. (color online) Cu clusters formed in Fe–3%Cu–4%Ni alloy after having aged at 1100 K. (Purple and cyan spheres respectively represent Cu and Ni atoms unless otherwise stated).

The cluster marked in Fig. 3 is analyzed by tracking the pathways of its constituent Cu and Ni atoms, and then the formation process is obtained as shown in Fig. 4. Small clusters are observed at $t = 0$ ns (Fig. 4(a)). They form in the equilibrium process, or they are some small-volume solute-rich regions formed by over-saturated solution atoms. Cu and Ni atoms locally gather into more small clusters, and these small clusters act as precipitation precursors. Small clusters are combined into big ones by Cu–Cu and Cu–Ni interactions, as shown in Fig. 4(b). As the process is further promoted, the Cu-rich cluster gradually grows up. Generally, the above process can be described by the fact that large Cu-rich cluster grows from small and subcritical clusters. The Cu-rich cluster departs and re-forms at $t = 73.8$ ns (Fig. 4(c)), $t = 130$ ns (Fig. 4(d)) and by the one that departs again at $t = 186.2$ ns (Fig. 4(e)). The Cu-rich cluster which is coagulated from two clusters by Ni atoms is clearly shown from Fig. 4(e) to Fig. 4(f). Ni atoms are excluded from Cu-rich cluster during cluster growth and ultimately form a shell structure located around the Cu-rich core. This is in good agreement with the core-shell structures observed in the experiment. The core-shell structures are formed due to the fact that Ni atoms in the cluster have a strong tendency to form Fe–Ni bonds,[39] and Ni is rejected from Cu-rich cluster to the interface between Cu-rich cluster and Fe-matrix over time.

In general, the formation of a Cu-rich cluster could be confirmed to experience three stages (Fe atoms have not been considered): (i) Cu and Ni atoms locally gather to form small clusters, and small clusters act as the precipitation precursors; (ii) small and mobile clusters are combined into big ones but with loose structures; and, (iii) Ni atoms are rejected to the interface between Cu-rich cluster and Fe-matrix to form core-shell structures during the growth.

The formation of Cu-rich cluster is probed by the pair distribution functions from the statistical point of view. The partial pair distribution functions of Cu–Cu, Cu–Ni, and Ni–Ni are shown in Fig. 5. The first peak values of $g_{\mathrm{Cu\text{–}Cu}}(r)$, $g_{\mathrm{Cu\text{–}Ni}}(r)$, and $g_{\mathrm{Ni\text{–}Ni}}(r)$ are almost the same at $t = 0$ ns. All the first peak values of $g_{\mathrm{Cu\text{–}Cu}}(r)$ increase significantly at

$t = 50$ ns, $t = 73.8$ ns, and $t = 186.2$ ns, which indicates that a growing number of Cu atoms are enriched in these durations. The increases of the second and third peak values of $g_{\text{Cu–Cu}}(r)$ at $t = 200$ ns indicate that the second and third nearest neighbor have the enrichment features of Cu. This result also validates the accuracy of the cut-off radius being set to be 4.0 Å. The data obtained by the pair distribution functions correspond well with the formation of Cu-rich clusters shown in Fig. 4. Nonetheless, the first peak value of $g_{\text{Cu–Ni}}(r)$ is larger than that of $g_{\text{Ni–Ni}}(r)$, inferring that Ni tends to be more favorable for aggregation with Cu than with itself. Ni prefers to be located around the Cu-rich clusters instead of forming Ni clusters.

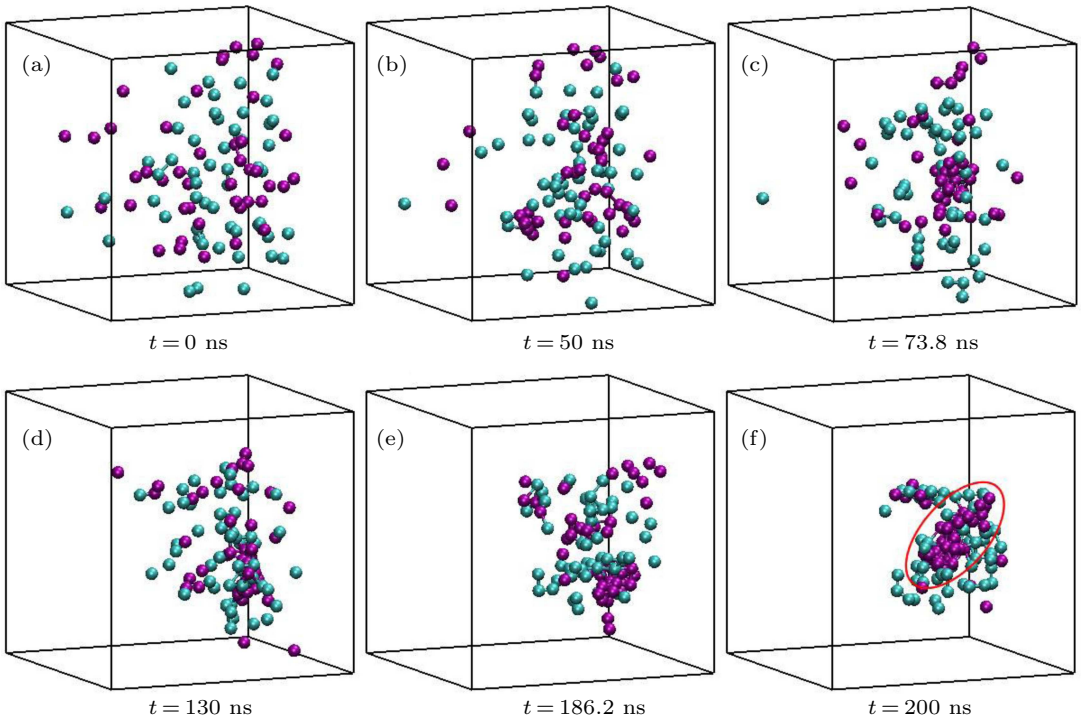


Fig. 4. (color online) Formation of Cu-rich clusters in Fe–3%Cu–4%Ni alloy aging at 1100 K. Fe atoms are not displayed for clarity.

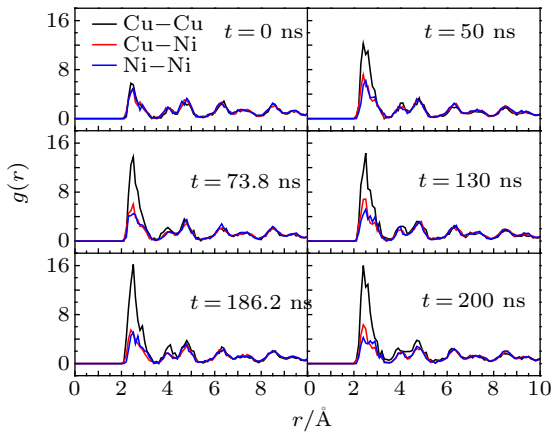


Fig. 5. (color online) Partial pair distribution functions $g_{\text{Cu–Cu}}(r)$, $g_{\text{Cu–Ni}}(r)$, and $g_{\text{Ni–Ni}}(r)$ of Fe–3%Cu–%4Ni alloys aging at 1100 K for different times.

The Cu-rich cluster grows at the expense of small clusters, as discussed in Fig. 4. When tracking trajectories of Ni atoms, a lot of situations are found where the Ni atoms are prone to combine small clusters into big ones, which is not enumerated in this article. Only a few examples are chosen to provide some details in Fig. 6. The negative mixing enthalpy of NiCu alloy indicates that forming a Cu–Ni bond is easier than forming Cu–Cu.[40] The presence of Ni atoms at the interface between Cu-rich clusters and Fe-matrix interface can significantly reduce system energy. Ni atoms prefer to interact with Cu atoms, and through Cu–Ni or Cu–Cu interaction small clusters can be merged into big ones and the growth of Cu-rich clusters is achieved. It is demonstrated that the presence of Ni promotes the nucleation of clusters containing vacancies and Cu, which is in agreement with experimental observations and the results of atomic kinetic Monte Carlo simulations.[24] In general, Ni plays an important role in the growth of Cu-rich clusters but the influence of Ni is reduced on later process of Ni rejection from core to interface. Thus, the influence of Ni on Cu precipitation is significant at the initial stage but it becomes weak in the later process.

3.2. First-principles calculations

First-principles calculations are employed to verify the results of MD simulations that Ni promotes small Cu-rich clusters to grow into big ones. The interactions between Cu clusters and Ni atoms in bcc Fe-matrix are studied by com-

paring the total energies of 54-atom supercells. It is defined that clusters are self-existent when the distance between them exceeds 4 Å, which is the same as cut-off radius in MD simulation. If all the possible configurations of clusters and Ni atoms must be checked, a tremendous number of calculations are required. Therefore, by simplifying Fig. 6, three sets of models are set to investigate the preferable sites of Ni atoms to determine whether Ni atoms are energetically prone to connecting small clusters.

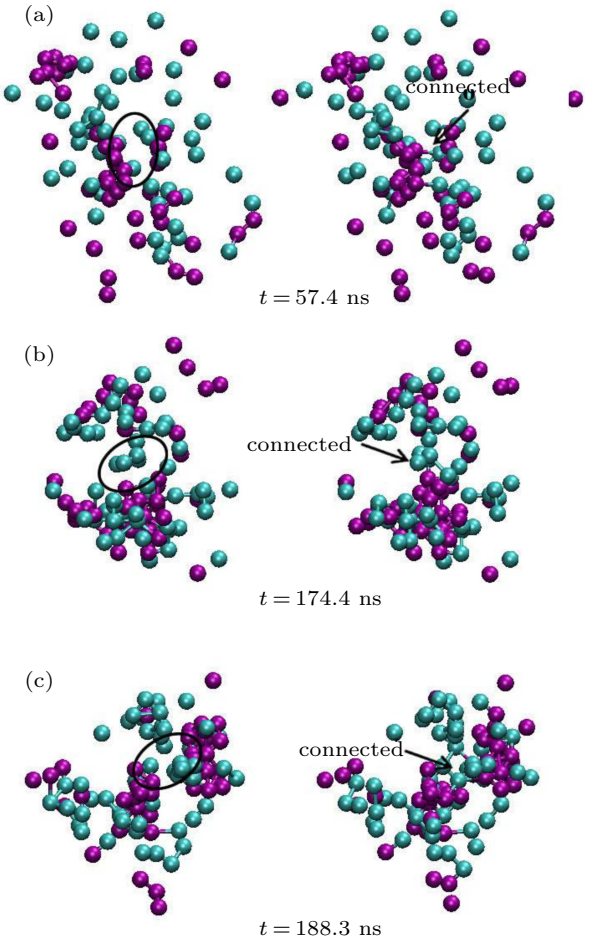


Fig. 6. (color online) Small clusters are combined into big ones by Ni atoms in the formation of Cu-rich clusters, and panels (a)–(c) show the results of a few examples at different times.

The configurations of Cu clusters are constant and those of Ni atoms are varying, as shown in Fig. 7. In model A, in case 1 two Ni atoms are located at the edge of Cu clusters; in case 2 two Ni atoms are located at the connection positions of two Cu clusters. In model B, in case 1 three Ni atoms are scattered around Cu clusters; in case 2 three Ni atoms are located at the combination positions. In model C, smaller sizes of clusters are designed to be a supplement to the models above: in case 1 two Ni atoms are in two clusters, respectively; in case 2 two Ni atoms are located at the connection positions of two Cu clusters. The total energies are listed in Table 1 in which shown are the energies of 54-atom super-cells in case 1 and case 2 of models A, B, C.

Systems with lower energies have better structural stabilities. In each group of models, the energies in case 2 that Ni atoms are located at connection positions between clusters are lowered by 0.65517, 0.43162, and 0.19526 eV, respectively. This infers that Ni atoms energetically prefer to combine small Cu-rich clusters into big ones. The stability of the system can also be reflected by the density of states (DOS) of Fermi level in Fig. 8. It is shown that the less the DOS at the Fermi level of an alloy, the more stable it is. Therefore, one can infer from the DOS that Ni atoms placed in connection points will result in a more stable structure than other configurations, which is consistent with the energetic properties obtained in Table 1. Thus, Ni atoms are energetically preferable to be at connection positions.

Table 1. The total energies of 54-atom supercells in case 1 and case 2 of models A, B, C.

Terms	$\Delta E = E_2 - E_1$		
	E_1/eV	E_2/eV	ΔE/eV
A	−379.41294	−380.06811	−0.65517
B	−376.97322	−377.40484	−0.43162
C	−403.18224	−403.37751	−0.19526

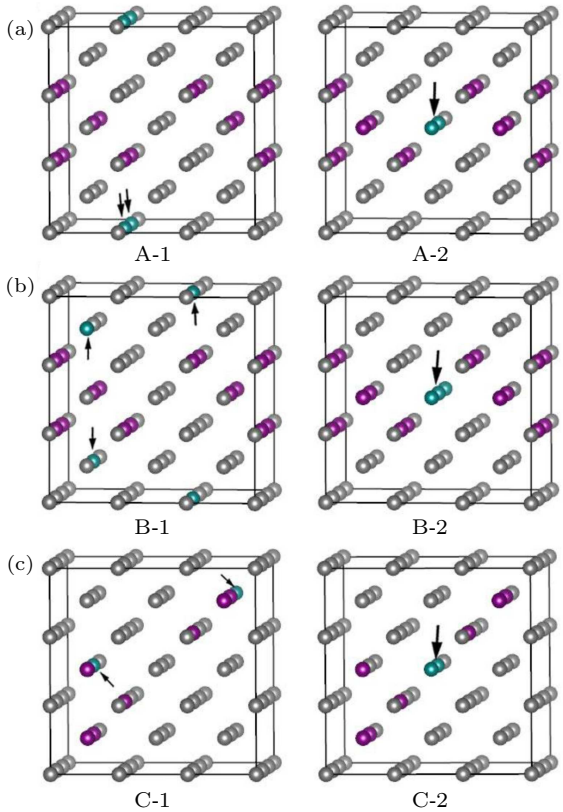


Fig. 7. (color online) Crystal structures of models A, B, and C in their unrelaxed forms. In each set of models, configurations of Ni atoms in case 1 and case 2 are different (Silver, purple, and cyan spheres represent Fe, Cu, and Ni atoms, respectively.

Vincent *et al.*'s calculations showed that Cu–Ni pair interaction energy is lower than that of Cu–Cu in the first nearest neighbors, but almost equals that in the second nearest neighbors.[41] The interaction between the second nearest neighbors is relatively weak, so that the number of Cu–Ni pair

interactions in the first nearest neighbors is mainly concerned. The number of the first nearest neighbors Cu–Ni interactions in case 2 of all models are larger than that in case 1, so that the total energies of case 2 is lower than those of case 1. In summary, Ni atoms at the connection points of two clusters lead to a decrease in the total energy of models.

At this point, it can be summarized that one of the reasons that Ni promotes Cu-rich precipitation is that Ni atoms promote small clusters to become big ones playing a connection role, and the nature is that Ni atoms energetically prefer to stay at the connection points among clusters.

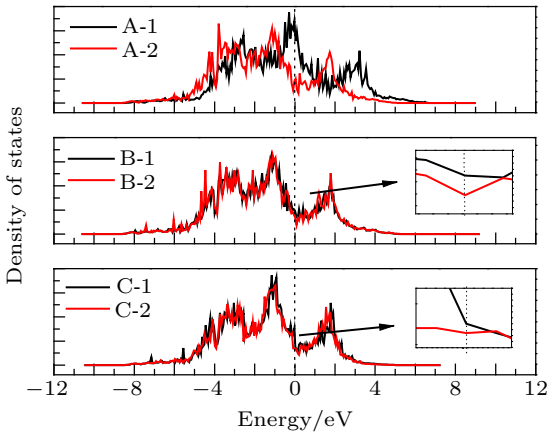


Fig. 8. (color online) Calculated spin-polarized total DOSs of models A, B, and C. The vertical dotted lines represent the Fermi level.

4. Conclusion

In this article, the early Cu precipitation is studied by MD simulations in Fe–3%Cu and Fe–3%Cu–4%Ni ternary alloys aging at 823 K and 1100 K. The formation sequence of Cu-rich cluster can be concluded as follows: small Cu-rich clusters are gathered into big ones forming core-shell structure that Ni shell surrounds Cu clusters.

The diffusion of Cu atoms is accelerated, and small clusters are promoted to grow into big ones by Ni atoms. That Ni atoms energetically prefer to stay at combination positions between clusters is verified by the first-principles calculations. A large number of the first nearest neighbor Cu–Ni interactions leads to a decrease of the total system energy.

Acknowledgment

The authors thank the Ziqiang Supercomputer Center at Shanghai University for providing us with high performance computing resources.

References

[1] Vaynman S, Isheim D, Kolli R P, Bhat S P, Seidman D N and Fine M E 2008 *Metall. Mater. Trans. A* **39** 363
[2] Zhang Z, Liu C, Wen Y, Hirata A, Guo S, Chen G, Chen M W and Chin B A 2012 *Metall. Mater. Trans. A* **43** 351
[3] Nagai Y, Tang Z, Hassegawa M, Kanai T and Saneyasu M 2001 *Phys. Rev. B* **63** 134110
[4] Odette G R and Lucas G E 2001 *JOM* **53** 18
[5] Odette G R and Lucas G E 1998 *Radiat. Eff. Defects Solids* **144** 189
[6] Knott J and English C 1999 *Int. J. Press. Vessels Pip.* **76** 891
[7] Auger P, Pareige P, Welzel S and Duysen J V 2000 *J. Nucl. Mater.* **280** 331
[8] Xu G, Chu D F, Cai L L, Zhou B X, Wang W and Peng J C 2011 *Acta Metall Sin.* **47** 905 (in Chinese)
[9] Yu X M and Zhao S J 2013 *Acta Metall Sin.* **49** 569 (in Chinese)
[10] Liu Q D and Zhao S J 2012 *MRS Commun.* **2** 127
[11] Liu Q D and Zhao S J 2012 *Metall. Mater. Trans. A* **44** 163
[12] Odette G R and Wirth B D 1997 *J. Nucl. Mater.* **251** 157
[13] Osetsky Y N and Serra A 1997 *Philos. Mag. A* **75** 1097
[14] Bouar Y L 2001 *Acta Mater.* **49** 2661
[15] Soisson F and Fu C C 2007 *Phys. Rev. B* **76** 214102
[16] Al-Motasem A T, Posselt M, Bergner F and Birkenheuer U 2011 *J. Nucl. Mater.* **414** 161
[17] Molnar D, Mukherjee R, Choudhury A, Mora A, Binkele P, Selzer M, Nestler B and Schmauder S 2012 *Acta Mater.* **60** 6961
[18] Hu L J, Zhao S J and Liu Q D 2012 *Mater. Sci. Eng. A* **556** 140
[19] Gao N, Wei K F, Zhang S X and Wang Z G 2012 *Chin. Phys. Lett.* **29** 096012
[20] Miller M K, Pareige P and Burke M G 2000 *Mater. Charact.* **44** 235
[21] Miller M K and Russell K F 2007 *J. Nucl. Mater.* **371** 145
[22] Osamura K, Okuda H, Asano K, Furusaka M, Kishida K, Kurosawa F and Uemoriet R 1994 *ISIJ Int.* **34** 346
[23] Zhang C and Enomoto M 2006 *Acta Mater.* **54** 4183
[24] Al-Motasem A T, Posselt M and Bergner F 2011 *J. Nucl. Mater.* **418** 215
[25] Seko A, Odagaki N, Nishitani S R, Tanaka I and Adachi H 2004 *Mater. Trans.* **45** 1978
[26] Wang Y, Hou H Y, Liu X B, Wang R S and Wang J T 2012 arXiv: 1212.6900 [hep-ph]
[27] Bonny G, Pasianot R C, Castin N and Malerba L 2009 *Philos. Mag.* **89** 3531
[28] Plimpton S 1995 *J. Comput. Phys.* **117** 1
[29] William H, Andrew D and Klaus S 1996 *J. Mol. Graphics* **14** 33
[30] Hyde J M, Marquis E A, Wilford K B and Williams T J 2011 *Ultramicroscopy* **111** 440
[31] Kohn W and Sham L J 1965 *Phys. Rev.* **140** A1133
[32] Kresse G and Furthmüller J 1996 *Phys. Rev. B* **54** 11169
[33] Kresse G and Joubert D 1999 *Phys. Rev. B* **59** 1758
[34] Wang Y and Perdew J P 1991 *Phys. Rev. B* **44** 13298
[35] Perdew J P, Chevary J A, Vosko S H, Jackson K A, Pederson M R, Singh D J and Fiolhais C 1992 *Phys. Rev. B* **46** 6671
[36] Marian J, Wirth B D, Odette G R and Perlado J M 2004 *Comput. Mater. Sci.* **31** 347
[37] Ju Y Y, Zhang Q M, Gong Z Z and Ji G F 2013 *Chin. Phys. B* **22** 083101
[38] Kittel C and McEuen P 1996 *Introduction to Solid State Physics*, 8th edn. (New York: Wiley) p. 37
[39] Murthy A S, Medvedeva J E, Isheim D, Lekakh S L, Richards V L and Van Aken D C 2012 *Scripta Mater.* **66** 943
[40] Xie Y P and Zhao S J 2011 *Comput. Mater. Sci.* **50** 2586
[41] Vincent E, Becquart C S and Domain C 2006 *J. Nucl. Mater.* **351** 88